Alkylation of [Pt2(μ-S)2(PPh3)4] with boronic acid derivatives

Oguejiofo T. Ujam, Ogochukwu E. Offie, Allen G. Oliver, Joshua I. Ume, Rhonda L. Stoddar, and J. Scott Mclndoe

August 2016

http://dx.doi.org/10.1080/00958972.2016.1226503

Correspondence to:
Dr. Oguejiofo T. Ujam
Department of Pure and Industrial Chemistry
University of Nigeria, Nsukka 410001, Enugu State, Nigeria.
e-mail: oguejiofo.ujam@unn.edu.ng
Phone: +2348062573097

Alkylation of $[Pt_2(\mu\text{-}S)_2(PPh_3)_4]$with boronic acid derivatives

Oguejiofo T. Ujam*[ab], Ogochukwu E. Offie[a], Allen G. Oliver[b], Joshua I. Ume[c], Rhonda L. Stoddard,[b] and J. Scott Mclndoe[b]

a. Department of Pure and Industrial Chemistry, University of Nigeria, Nsukka 410001, Enugu State, Nigeria.
b. Department of Chemistry and Biochemistry, University of Notre Dame, Notre Dame, IN 46556, USA.
c. Department of Mechanical Engineering, University of Nigeria, Nsukka 410001, Enugu State, Nigeria.
d. Department of Chemistry, University of Victoria, P. O. Box 3065, Victoria, BC V8W 3V6, Canada.

Correspondence: e-mail: oguejiofo.ujam@unn.edu.ng; Phone: +2348062573097

Abstract

The reactivity of the metalloligand $Pt_2(\mu\text{-}S)_2(PPh_3)_4$ with the boron-functionalized alkylating agents $BrCH_2(C_6H_4)B(OR)_2$ (R = H or CMe_2) was investigated by electrospray ionization mass spectrometry (ESI-MS) in real time using the pressurized sample infusion (PSI). The macroscopic reaction of $Pt_2(\mu\text{-}S)_2(PPh_3)_4$ with one mole equivalent of alkylating agents $BrCH_2(C_6H_4)B\{OC(CH_3)_2\}_2$ and $BrCH_2(C_6H_4)B(OH)_2$ gave the dinuclear monocationic μ-sulfide thiolate complexes $[Pt_2(\mu\text{-}S)\{\mu\text{-}SCH_2(C_6H_4)B\{OC(CH_3)_2\}_2\}(PPh_3)_4]^+$ and $Pt_2(\mu\text{-}S)\{\mu\text{-}S^+CH_2(C_6H_4)B(OH)(O^-)\}(PPh_3)_4$. The products were isolated as the $[PF_6]^-$ salts and zwitterion respectively, and fully characterized by ESI-MS, IR, ^1H and ^{31}P NMR spectroscopy and single crystal X-ray structure determinations.

Keywords: real time analysis, mass spectrometry, platinum complexes, alkylation, boronic acid.

Introduction

The applied coordination chemistry of the neutral dinuclear platinum metalloligand, $Pt_2(\mu\text{-}S)_2(PPh_3)_4$ **1** has continued to attract considerable interest due to its catalytic potential [1] and as a precursor for the synthesis of organosulfur compounds.[2] The bridging sulfides are electron-rich and the reactivity towards metal fragments has been exploited in the synthesis of multimetallic aggregates.[3-11] Alkylation reactions of **1** with mild electrophiles was realised in the early preliminary studies.[12-15] Recently, the rudimentary reactivity of **1** with simple mild alkylating agents[13] has been extended to functionalized alkylating agents (electrophiles).[16, 17] The alkylation of **1** provides a facile route for the generation of functionalized thiolate ligands bonded to platinum, $[Pt_2(\mu\text{-}S)(\mu\text{-}SR)(PPh_3)_4]^+$, $[Pt_2(\mu\text{-}SR)(\mu\text{-}SR)(PPh_3)_4]^{2+}$ and $[Pt_2(\mu\text{-}SR')(\mu\text{-}SR)(PPh_3)_4]^{2+}$ (R = functionalized organic group)[17-20] including a zwitterion $[Pt_2(\mu\text{-}S)\{\mu\text{-}S(CH_2)_3SO_3\}(PPh_3)_4]$.[21] An electrospray ionization mass spectrometry (ESI-MS) based screening of the reactions of **1** with a variety of alkylating agents indicates the possibility of generating dinuclear platinum complexes containing a range of thiolate ligands.[16] This methodology has been used to generate coordinated functionalized thiolate ligands (-SR) on **1**.[17] Notably, any desired functionality can be incorporated into **1** through a suitable electrophile.

The ability to incorporate any functional group into **1** means that the chemical application of the generated thiolate complex, $[Pt_2(\mu\text{-}S)(\mu\text{-}SR)(PPh_3)_4]^+$ can be streamlined. In synthetic chemistry, coordinated sulfide ligands should be a facile precursor to thiolate complexes but this is yet to be fully recognized and utilized for its importance.[22] Alkylated derivatives of **1** have the potential to act as cationic metalloligands. Derivatives $[Pt_2(\mu\text{-}S)(\mu\text{-}SR)(PPh_3)_4]^+$ (R = n-Bu or CH_2Ph) are able to coordinate organo-mercury (RHg^+) and phosphine-gold(I) (Ph_3PAu^+) cations through the underivatised sulfide ligand.[23] Interests in incorporating boron derivatives into **1** are drawn from the perspective that the resulting complex can be further derivatised with coordinated metallic centers or suitable organic moieties. Boronic acid have been used in the synthesis of bi- and polyaryl compounds via the Suzuki–Miyaura coupling reactions.[24-28] An incorporated boronic group on **1** could be used as a synthetic precursor to generating multinuclear metallic species through a Suzuki–Miyaura reaction. To date, no derivatives of **1** containing boron or any metalloid functionalized thiolate

ligands have been synthesized using sulfide alkylation. We present in this report the first synthesis and characterization of boronic acid derivatives of **1**. The isolation and crystallographic identification of the dinuclear structures incorporating boron thiolate substituents suggests that useful synthetic precursor groups can be incorporated into **1**, and in particular open up avenues for preparing larger multinuclear assemblies on the nanometer scale.

Results and Discussion

The products, rates of product formation, reaction completion time, and the rate of consumption of the starting materials was monitored utilizing the Pressurized Sample Infusion Electrospray Ionization Mass Spectrometry (PSI-ESI-MS) technique.[29, 30] The reaction mixture is prepared in a Schlenk flask into which a length of PEEK tubing attached to the source of the mass spectrometer is inserted. An overpressure of 2 - 4 psi is applied displacing the reacting solution into the MS. This allows for real-time observation of all charged species and how they behave over the course of the reaction,[31-34] and providing a better understanding of mechanism and optimization of synthetic protocols. For this report speciation and dynamic behavior in the reaction of **1** with 4-(bromomethyl)phenylboronic acid pinacol ester, $BrCH_2(C_6H_4)B\{OC(CH_3)_2\}_2$, **2** was monitored.

The alkylation reaction of $BrCH_2(C_6H_4)B\{OC(CH_3)_2\}_2$ **2** with **1** was determined to be second order (Figure 1), consistent with the expected S_N2 mechanism for an alkylation reaction. **1** disappeared rapidly with consequent formation of the monoalkylated cationic product, $[Pt_2(\mu\text{-}S)\{\mu\text{-}SCH_2(C_6H_4)B\{OC(CH_3)_2\}_2\}(PPh_3)_4]^+$, **2a**. This was indicated by the immediate appearance of the monoalkylated product peak at *m/z* 1720.6. The reaction was complete 6 minutes after injection. The two species $(\{[Pt_2(\mu\text{-}S)_2(PPh_3)_4] + H\}^+$ and $[Pt_2(\mu\text{-}S)\{\mu\text{-}SCH_2(C_6H_4)\ B\{OC(CH_3)_2\}_2\}(PPh_3)_4]^+$, **2a** have dramatically different ESI-MS responses due to the difference in their electrospray ionization efficiencies. $[Pt_2(\mu\text{-}S)_2(PPh_3)_4]$ produces weak $[\mathbf{1} + H]^+$ ions in methanol, but is immediately outcompeted by the appearance of the inherently charged alkylated product, which provides a much stronger ESI-MS response in addition to consuming **1**.

Syntheses and spectroscopic characterization

Halogeno-boronic acid compounds containing inactivated bromoalkyl ($BrCH_2$-) groups were selected for the synthesis due to the better leaving ability of bromide than chloride and

their lesser tendency to form dialkylated species. The laboratory scale reactions were monitored by ESI-MS[35] which has been previously found to be a valuable technique in the investigation of the alkylation chemistry of $[Pt_2(\mu\text{-}S)_2(PPh_3)_4]$[16]. **1** is a neutral species but is mono-protonated in methanol and detected in ESI-MS as $[\mathbf{1} + H]^+$, at *m/z* 1503.5. $\{[Pt_2(\mu\text{-}S)_2(PPh_3)_4] + H\}^+$ has been previously synthesized by reacting dilute HCl with **1**, isolated and characterized by single crystal X-ray crystallography[36]. The gradual change in colour from an orange methanolic suspension of **1** to a clear yellow solution indicated alkylation upon the addition of an electrophile. When a weaker electrophile is used monoakylation of **1** occurs generating the monocation $[Pt_2(\mu\text{-}S)(\mu\text{-}SR)(PPh_3)_4]^+$. The alkylating agent **2** reacted with **1** in methanol, within 6 min to give the monoalkylated product $[Pt_2(\mu\text{-}S)\{\mu\text{-}SCH_2(C_6H_4)(OC(CH_3)_2)_2\}(PPh_3)_4]^+$, **2a** (Scheme 1**)** which was isolated as the PF_6^- salt following the addition of excess NH_4PF_6. No dialkylated products were observed. The reaction of $BrCH_2(C_6H_4)B(OH)_2$, **3** with **1** within same time interval yielded three monocationic species that were detected by ESI-MS and assignable to the three alkylated products: $[Pt_2(\mu\text{-}S)\{\mu\text{-}SCH_2C_6H_5)(PPh_3)_4]^+$, *m/z* 1593.4 from the loss of $B(OH)_2$ moiety; a hemiketal-like species $[Pt_2(\mu\text{-}S)\{\mu\text{-}SCH_2(C_6H_4)B(OH)(OCH_3)\}(PPh_3)_4]^+$, *m/z* 1651.5 and $[Pt_2(\mu\text{-}S)\{\mu\text{-}SCH_2(C_6H_4)OH\}(PPh_3)_4]^+$, *m/z* 1609.5. The minor peak at *m/z* 538.3 is $[N(PPh_3)_2]^+$, bis(triphenylphosphoranylidnene)ammonium, which is the internal standard (Figure 2). The masses were identified by comparing the experimental isotope patterns with calculated ones.[37] No peak was observed in the mass spectrum that was attributable to the formation of the expected product $[Pt_2(\mu\text{-}S)\{\mu\text{-}SCH_2(C_6H_4)B(OH)_2\}(PPh_3)_4]^+$. The ESI-MS of the products isolated as $[PF_6]^-$ salts also gave the same *m/z* species in the positive ion mode. Purification by vapor diffusion of diethyl ether into the dichloromethane solution of the products yielded crystals suitable for single crystal X-ray structure determination and further spectroscopic characterization. The structural determination showed that the compound formed was a zwitterion (neutral complex) $Pt_2(\mu\text{-}S)\{\mu\text{-}S^+CH_2(C_6H_4)B(OH)(O^-)\}(PPh_3)_4$; accordingly, $[PF_6]^-$ was not observed in the crystal structure. $Pt_2(\mu\text{-}S)\{\mu\text{-}S^+CH_2(C_6H_4)B(OH)(O^-)\}(PPh_3)_4$ is a neutral species and as such not detectable by ESI-MS.

The monoalkylated complexes, **2a·(PF$_6$)** and **3a** show IR, ^1H and $^{31}P\{1H\}$ NMR spectroscopic features expected for these type of complexes. The differences between the IR absorption bands of the reactants $\{[Pt_2(\mu\text{-}S)_2(PPh_3)_4]$ **1**, alkylating agents **2** ,**3**$\}$ and the products **2a·(PF$_6$)** and **3a** clearly indicate the incorporation of the boronic acid electrophile into **1**. The assignment of the IR bands is comparable with those reported in the literature[38]. In the IR spectrum, the OH vibration (3336 cm^{-1}) in **3** shifted to 3435 cm^{-1} in **3a.** The absorption bands

of the B-O bond in **2** (1355 cm^{-1}) and **3** (1350 cm^{-1}) shifted to 1360 cm^{-1} and 1367 cm^{-1} in **2a·(PF_6)** and **3a** respectively.

Predictably, the ^1H NMR spectra showed a complicated set of resonances in the aromatic region due to the terminal triphenylphosphine ligands and were broadly assigned as such. However, SCH_2 hydrogen atoms were easily identified as broad peaks at δ 3.59 ppm and 3.60 ppm for **2a·(PF_6)** and **3a**, respectively. The observation of this resonance is further indication of sulfide alkylation. In both complexes, there are two inequivalent phosphorus centers: the phosphorus *trans* to the thiolate (-SR) or and the phosphorus *trans* to the sulfide (-S-) atom. The $^{31}P\{^1H\}$ NMR spectra showed nearly superimposed central resonances and clearly separated satellite peaks due to ^{195}Pt coupling (Figure 3). The $^1J(PtP)$ coupling constants showed the differences due to the *trans* influences of the substituted and the unsubstituted sulfide centers.[39] The *trans* influence of the unsubstituted sulfide is greater than the thiolate (substituted) species demonstrated by the coupling constants at (2630 and 3290 Hz) for **2a·(PF_6)** and (2630 and 3270 Hz) **3a**, respectively.

X-ray structures of the complexes $[Pt_2(\mu\text{-}S)\{\mu\text{-}SCH_2(C_6H_4)(OC(CH_3)_2)_2\}(PPh_3)_4](PF_6)$, **2a·($PF_6$)** and $[Pt_2(\mu\text{-}S)\{\mu\text{-}S^+CH_2(C_6H_4)B(OH)(O^-)\}(PPh_3)_4]$, **3a** were determined to confirm the identity of complexes and to allow for structural comparison with related monoalkylated molecules previously reported. Selected bond lengths and angles are presented in Tables 1 and 2. The molecular structures and atom numbering schemes for **2a·(PF_6)** and **3a** are shown in Figures 4 and 5 respectively. The structures show both complexes **2a·(PF_6)** and **3a** have the typical hinged conformation of the $\{Pt_2(\mu\text{-}S)_2\}$ core dihedral angles formed by the two PtS_2 planes in each of **2a·(PF_6)** and **3a** of 136.66° and 134.40°, respectively. A comparison of the important structural parameters of **2a·(PF_6)** and **3a** with those of structurally-related monoalkylated compounds $[Pt_2(\mu\text{-}S)\{\mu\text{-}SCH_2C(O)Ph\}(PPh_3)_4](BPh_4)$[17] **4a·($BPh_4$)**, $[Pt_2(\mu\text{-}S)\{\mu\text{-}SCH_2C(=NNHC(O)NH_2)Ph\}(PPh_3)_4](PF_6)$[17] **5a·($PF_6$)** and $[Pt_2(\mu\text{-}S)\{\mu\text{-}SCH_2CH_2NHC(O)N(CH_2CH_2)_2S\}(PPh_3)_4](PF_6)$[17] **6a·($PF_6$)** are shown in Table 5. The structural parameters are comparable across the series of compounds.

Experimental

Materials and Instrumentation

The alkylating agents $BrCH_2(C_6H_4)B(OH)_2$, $BrCH_2(C_6H_4)B\{OC(CH_3)_2\}_2$ (CAUTION! Highly toxic, potent lachrymator and vesicant and should be handled using appropriate safety

precautions) and $PtCl_2(PPh_3)_2$, $Na_2S{\cdot}9H_2O$ and NH_4PF_6 were supplied by Sigma-Aldrich. Reaction solvents: Benzene (Sigma-Aldrich), methanol (Caledon Chemicals), dichloromethane (Sigma-Aldrich) and diethyl ether (EMD Chemicals) were of laboratory reagent grade and used without further purification. $[Pt_2(\mu\text{-}S)_2(PPh_3)_4]$ **1** was synthesized according to the literature procedure by the metathesis reaction of *cis*-$PtCl_2(PPh_3)_2$ with $Na_2S{\cdot}9H_2O$ in benzene[13, 40].

NMR spectra were recorded in $CDCl_3$ solution, unless otherwise stated. ^1H and $^{31}P\{^1H\}$ spectra referenced to TMS for ^1H and to 85% phosphoric acid for ^{31}P were recorded on Bruker Avance 300 MHz spectrometer. IR spectra were obtained as KBr disks with a Perkin Elmer Spectrum FTIR Spectrometer, version 10.4.3. Melting points of the compounds were determined with a Gallenkamp melting point apparatus and are uncorrected. ESI-MS of solid products were obtained by dissolving a small quantity of the material in 1–2 drops of dichloromethane, followed by dilution to ca. 2 mL using methanol. ESI-MS kinetic profile of the reactions was analyzed by the Pressurised Sample Infusion (PSI) technique. Mass Spectral data were recorded on a Waters Micromass Q-TOF II Mass Spectrometer in positive ion mode using pneumatically assisted electrospray ionization: capillary voltage, 2900 V; sample cone voltage, 15 V; extraction voltage, 1 V; source temperature, 80 °C; desolvation temperature, 160 °C; cone gas flow, 100 L h^{-1}; desolvation gas flow, 100 L h^{-1}; collision voltage, 2 V; MCP voltage, 2400 V. No smoothing of the data was performed and comparison of observed and calculated isotope patterns[37] was used in the ion assignment.

Pre-synthetic kinetic profile of the reaction of $[Pt_2(\mu\text{-}S)_2(PPh_3)_4]$ with $BrCH_2(C_6H_4)B\{OC(CH_3)_2\}_2$

Minuscule amounts of the two reactants **1** (7 mg, 0.0047 mmol) and $BrCH_2(C_6H_4)B\{OC(CH_3)_2\}_2$, **2** (1.4 mg, 0.0047 mmol, 1.2 mol equiv.) were used for PSI-ESI-MS investigations. The reaction solvent (methanol) was sparged with nitrogen on the Schlenk line for 2 h to remove oxygen. The $[Pt_2(\mu\text{-}S)_2(PPh_3)_4]$ **1** was added to the Schlenk flask and purged with argon for 30 min. The electrophile, $BrCH_2(C_6H_4)B\{OC(CH_3)_2\}_2$, **2** in a sample vial capped with a septum was sparged with nitrogen on the Schlenk line for 30 min. A methanolic solution of **1** was initially injected by PSI into ESI-MS. Once the signal for $[\mathbf{1} + H]^+$ at *m/z* 1503.5 reached a stable intensity, a 1 mL methanol solution of $BrCH_2(C_6H_4)B\{OC(CH_3)_2\}_2$ **2** was added to the reaction mixture by direct injection into the reaction flask and reaction data recorded by the mass spectrometer.

Synthesis of $[Pt_2(\mu\text{-}S)\{\mu\text{-}CH_2(C_6H_4)B\{OC(CH_3)_2\}_2\}(PPh_3)_4](PF_6)$, 2a·$(PF_6)$

To an orange suspension of **1** (50 mg, 0.033 mmol) in methanol (25 mL) was added an excess of $BrCH_2(C_6H_4)B\{OC(CH_3)_2\}_2$ (10 mg 0.037 mmol, 1.1 mole equiv.) and the solution stirred for 45 min at room temperature. Complete formation of the monoalkylated product was confirmed by ESI-MS which showed $[Pt_2(\mu\text{-}S)\{\mu\text{-}SCH_2(C_6H_4)B\{OC(CH_3)_2\}_2\}(PPh_3)_4]^+$ at *m/z* 1720.57. The solution was filtered and excess NH_4PF_6 (25 mg, 0.15 mmol) added to the clear filtrate. The resulting yellow precipitate was filtered, washed with water (4 × 10 mL) and diethyl ether (4 × 10 mL) and dried in air, giving **2a·(PF_6)** (54 mg, 87%). Crystals suitable for X-ray structure determination were isolated by slow diffusion of diethyl ether into a dichloromethane solution of **2a·(PF_6)**.

M.p.: 168–170 ºC.

IR: 840, 1096, 1144, 1360, 1436, 1481, 1610, 3054, 3441 cm^{-1}.

$^{31}P\{^1H\}$ NMR ($CDCl_3$): δ 24.5 [d, $^1J(PtP_B)$, 3291, P_B], 22.88 [d, $^1J(PtP_A)$, 2628.19, P_A], $^2J(P_AP_B)$, 30.

^1H NMR ($CDCl_3$, 300 MHz): δ 7.52–6.63 (64H, m, 17Ph), 3.59 (2H, t, SCH_2) 1.34 (9H, s, CH_3)

ESI-MS (*m/z*): ($[M]^+$ 100%). 1720.6

Synthesis of $Pt_2(\mu\text{-}S)\{\mu\text{-}S^+CH_2(C_6H_4)B(OH)(O^-)\}(PPh_3)_4$, 3a

To a suspension of **1** (50 mg, 0.033 mmol) in methanol (25 mL) was added an excess of $BrCH_2CH_2(C_6H_4)B(OH)_2$ (7.9 mg, 0.037 mmol, 1.1 mole equiv.) and the solution stirred for 30 min at room temperature. Complete formation of the monoalkylated products was confirmed by ESI-MS which showed $[Pt_2(\mu\text{-}S)(\mu\text{-}SCH_2C_6H_5)(PPh_3)_4]^+$, *m/z* 1593.4, $[Pt_2(\mu\text{-}S)\{\mu\text{-}SCH_2(C_6H_4)OH\}(PPh_3)_4]^+$, *m/z* 1609.5 and $[Pt_2(\mu\text{-}S)\{\mu\text{-}SCH_2(C_6H_4)B(OH)(OCH_3)\}(PPh_3)_4]^+$, *m/z* 1651.5. The solution was filtered and NH_4PF_6 (25 mg, 0.15 mmol) added to the clear filtrate. The resulting yellow precipitate was filtered, washed with water (4 × 10 mL) and diethyl ether (4 × 10 mL) and dried in air, giving (52 mg, 87%) of the product. Recrystallisation by vapour diffusion of hexane into a chloroform solution of **3a** gave pure crystals of $[Pt_2(\mu\text{-}S)\{\mu\text{-}S^+CH_2(C_6H_4)B(OH)(O^-)\}(PPh_3)_4]$ suitable for X-ray structure determination and spectroscopic characterisations.

M.p.: 158–160 ºC.

IR: 1096, 1186, 1367, 1435, 1481, 1608, 3052, 3435 cm^{-1}.

$^{31}P\{^{1}H\}$ NMR ($CDCl_3$): δ 23.50 [d, $^{1}J(PtP_B)$, 3272.51, P_B], 23.05 [d, $^{1}J(PtP_A)$, 2632.04, P_A], $^{2}J(P_AP_B)$, 36.

^{1}H NMR ($CDCl_3$, 300 MHz): δ 7.55–6.61 (64H, m, 17Ph), 3.60 (2H, t, SCH_2), 1.58 (H, s, OH)

X-ray structure determinations of 2a·(PF_6) and 3a

An appropriately sized crystal of **2a·(PF_6)** or **3a** was selected from a bulk sample under Paratone-N oil and mounted on a MiTeGen loop. The loop was transferred to a Bruker APEX-II diffractometer equipped with a CCD area detector under a cold gaseous nitrogen stream. An arbitrary sphere of data was recorded, using Mo-Kα radiation (λ 0.71073 Å) and a combination of ω- and φ-scans of 0.5°[41]. Data were corrected for absorption and polarization effects and analyzed for space group determination.[42] The structures were solved by intrinsic phasing methods and expanded routinely[43]. The models were refined by full-matrix least-squares analysis of F^2 against all reflections. All non-hydrogen atoms were refined with anisotropic atomic displacement parameters. Unless otherwise noted, hydrogen atoms were included in calculated positions. Atomic displacement parameters for the hydrogens were tied to the U_{eq} parameter of the atom to which they are bonded (1.5 × for methyl, 1.2 × for all others). Crystallographic data are summarized in Tables 3 and 4.

[Pt_2(μ-S){μ-SCH_2(C_6H_4)B{$OC(CH_3)_2$}$_2$}(PPh_3)$_4$][PF_6], 2a·(PF_6)

The complex crystallizes as colourless block-like crystals from vapour diffusion of diethyl ether into a dichloromethane solution at room temperature. There are four molecules of the $[Pt_2(\mu\text{-}S)\{\mu\text{-}SCH_2(C_6H_4)B\{OC(CH_3)_2\}_2\}(PPh_3)_4]^+$ cation, four associated PF_6^- anions and twelve dichloromethane molecules of crystallization in the unit cell of the primitive, centrosymmetric, monoclinic and are uncorrected $P2_1/c$. The structure of **2a·(PF_6)** complex is as expected. The cation consists of two, four-coordinate, square planar Pt centers; each is coordinated by two triphenylphosphine ligands and bridged by a sulfide sulfur and the thiol sulfur of the dioxaborolane phenyl methanethiol ligand (Figures 4 and Table 1). One of the three independent dichloromethane molecules located within the asymmetric unit is disordered. Two sites were observed for this molecule. Refinement of the occupancy of the two sites yielded an effective 50:50 occupancy. In the final model, the occupancies of the two sites were set to 50%. Further, one of the chlorine atoms is additionally disordered over two sites and was refined with 25% occupancy at each site.

$Pt_2(\mu\text{-}S)\{\mu\text{-}S^+CH_2(C_6H_4)B(OH)(O^-)\}(PPh_3)_4$, 3a

The compound $Pt_2(\mu\text{-}S)\{\mu\text{-}S^+CH_2(C_6H_4)B(OH)(O^-)\}(PPh_3)_4$, **3a** crystallizes as colorless block-like crystals from a chloroform/hexanes solution. There are four molecules of the complex in the unit cell of the primitive, centrosymmetric, monoclinic space group $P2_1/n$. Also present was diffuse, disordered solvent. After several attempts at modeling this electron density it was elected that the solvent contribution to the model be accounted for using the SQUEEZE routine in PLATON.[44] The routine located two voids, of 1182 $Å^{-3}$, each contributing 305 electrons to the intensities. These additional factors were omitted from the final model and no interpretation of the solvent content (likely to be less than unitary values for various combinations of solvents present from crystallization) made. The solvent content has not been added to the chemical formula.

The structure of **3a** is as expected (Figure 5, Table 2). The core consists of two Pt atoms each coordinated in a square-planar fashion. The coordination environment about each Pt center is two, *cis,* triphenylphosphine ligands, a bridging sulfur and the bridging sulfur of the thiolate ligand. There is some disorder present in the borate moiety that has been modeled with one fully occupied oxygen and two partial occupancy oxygen atoms. The boron is modelled with isotropic atomic displacement parameters. It is also slightly disordered, but not well defined in its disorder. Thus a reasonable model could not be obtained.

The disordered borate appears to consist of $B(OH)(O^-)$. Despite the disorder present in this group, the ordered oxygen, O1, has a slightly longer bond distance (B1-O1 = 1.446(18) Å) than the oxygen that is disordered over two sites (B1-O2/O2A = 1.29(2)/1.38(2) Å). This would support the negative charge for a zwitterionic species residing on this peripheral group, balancing the core positive (+) charge (from the two Pt centres, bridging S and bridging thiolate S).

Conclusions

This study has demonstrated the successful incorporation of two organo-boron moieties on to $\{Pt_2(\mu\text{-}S)_2\}$ core yielding dinuclear platinum complexes of the type, $[Pt_2(\mu\text{-}S)(\mu\text{-}SR)(PPh_3)_4]^+$ and a zwitterion $[Pt_2(\mu\text{-}S)(\mu\text{-}S^+R^-)(PPh_3)_4]$. Potentially, any boron group can be incorporated into **1** through a suitable electrophile and the unsubstituted sulfide center can be capped with a suitable group. In the future, we also intend to investigate alkylated boron derivatives in the synthetic design of diverse bi- and polyaryl compounds of **1**, especially in the preparation of assemblies containing multiple $\{Pt_2(\mu\text{-}S)_2\}$ cores.

Acknowledgements

JSM thanks NSERC (Discovery and Discovery Accelerator Supplement) for operational and infrastructural funding and CFI, BCKDF and the University of Victoria for infrastructural support. Eric Janusson (University of Victoria, Victoria, BC, Canada) is thanked for mass spectrometric support.

Supplementary material

Crystallographic data for the structures, **2a·(PF$_6$), 3a** described in this paper have been deposited with the Cambridge Crystallographic Data Centre, CCDC No. 1431797 and 1431798 respectively. Copies of the data can be obtained free of charge on application to The Director, CCDC, 12 Union Road, Cambridge CB2 1EZ, UK (Fax: +44-1223-336033; e-mail deposit@ccdc.cam.ac.uk or www: http://www.ccdc.cam.ac.uk).

References

1. S. H. Chong, A. Tjindrawan and T. S. A. Hor, *J. Mol. Catal. A: Chem*, 2003, **204–205,**, 267.
2. S. H. Chong, D. J. Young and T. S. A. Hor, *J. Organomet. Chem.*, 2006, **691**, 349.
3. S.-W. A. Fong and T. S. A. Hor, *J. Chem. Soc., Dalton Trans.*, 1999, 639.
4. W. Henderson and T. S. A. Hor, *Inorg. Chim. Acta*, 2010, **363**, 1859.
5. W. Henderson and A. G. Oliver, *Inorg. Chim. Acta*, 2011, **375**, 248.
6. S.-W. A. Fong, T. S. A. Hor, W. Henderson, B. K. Nicholson, S. Gardyne and S. M. Devoy, *J. Organomet. Chem.*, 2003, **679**, 24.
7. S.-W. A. Fong, T. S. A. Hor, S. M. Devoy, B. A. Waugh, B. K. Nicholson and W. Henderson, *Inorg. Chim. Acta*, 2004, **357**, 2081.
8. R. Mas-Ballesté, W. Clegg, A. Lledós and P. González-Duarte, *Eur. J. Inorg. Chem.*, 2004, 3223.
9. S. M. Devoy, W. Henderson, B. K. Nicholson, J. Fawcett and T. S. A. Hor, *Dalton Trans.*, 2005, 2780.
10. B. C. White, D. Harrison, W. Henderson, B. K. Nicholson and T. S. A. Hor, *Inorg. Chim. Acta*, 2010, **363**, 2387.

11. S.-W. A. Fong, W. T. Yap, J. J. Vittal, W. Henderson and T. S. A. Hor, *J. Chem. Soc., Dalton Trans.*, 2002, 1826.
12. J. Chatt and D. M. P. Mingos, *J. Chem. Soc. A,*, 1970, 1243.
13. R. Ugo, G. La Monica, S. Cenini, A. Segre and F. Conti, *J. Chem. Soc. (A)*, 1971, 522.
14. R. R. Gukathasan, R. H. Morris and A. Walker, *Can. J. Chem.*, 1983, 2490.
15. C. E. Briant, C. J. Gardner, T. S. A. Hor, N. D. Howells and D. M. P. Mingos, *J. Chem. Soc., Dalton Trans.*, 1984, 2645.
16. W. Henderson, S. H. Chong and T. S. A. Hor, *Inorg. Chim. Acta*, 2006, **359**, 3440.
17. O. T. Ujam, W. Henderson, B. K. Nicholson and T. S. A. Hor, *Inorg. Chim. Acta*, 2010, **363** 3558.
18. S. H. Chong, L. L. Koh, W. Henderson and T. S. A. Hor, *Chem. Asian. J.*, 2006, **1 –2**, 264
19. S. H. Chong, W. Henderson and T. S. A. Hor, *Dalton Trans.*, 2007, 4008.
20. O. T. Ujam, W. Henderson, B. K. Nicholson and T. S. A. Hor, *Inorg. Chim. Acta*, 2011, **376**, 255.
21. O. T. Ujam, W. Henderson and B. K. Nicholson, 2013, **54**, 523.
22. M. C. Gimeno, *Handbook of Chalcogen Chemistry*, Royal Society of Chemistry,Cambridge, 2007.
23. W. Henderson, B. K. Nicholson, S. M. Devoy and T. S. A. Hor, *norg.Chim.Acta* 2008, **361**, 1908.
24. N. Miyaura and A. Suzuki, *J. Chem. Soc. Chem. Commun.*, 1979, 866.
25. N. Miyaura, T. Yanagi and A. Suzuki, *Synth. Commun.*, 1981, **11**, 513.
26. N. Miyaura and A. Suzuki, *Chem. Rev.*, 1995, **95**, 2457.
27. A. Suzuki, in *Metal Catalysed Cross Coupling Reactions*, Wiley-VCH, Weinheim, Editon edn., 1997.
28. F. Diederich and P. J. Stang, eds., *Boronic Acids*, Wiley-VCH, Hall D, 2005.
29. K. L. Vikse, M. P. Woods and J. S. McIndoe, *organomettallics*, 2010, **29**, 6615–6618.
30. K. L. Vikse, Z. Ahmadi, J. Luo, N. van der Wal, Kevin Daze, N. Taylor and J. S. McIndoe, *Int. J. Mass Spectrom.*, 2012, **323–324**.
31. K. L. Vikse, M. A. Henderson, A. G. Oliver and J. S. McIndoe, *Chem. Commun.*, 2010, **46**, 7412.
32. K. Vikse, T. Naka, J. S. McIndoe, M. Besora and F. Maseras, *ChemCatChem*, 2013, **5**, 3604.

33. Z. Ahmadi and J. S. McIndoe, *Chem. Commun.*, 2013, **49**, 11488.
34. Z. Ahmadi, A. G. Oliver and J. S. McIndoe, *ChemPlusChem* 2013 **78** 632
35. W. Henderson and J. S. McIndoe (Eds.), *Mass Spectrometry of Inorganic, Coordination and Organometallic Compounds – Tools–Techniques–Tips, John*, Wiley & Sons, 2005.
36. S.-W. A. Fong, J. J. Vittal, W. Henderson, T. S. A. Hor, A. G. Oliver and C. E. F. Rickard, *Chem.Commun.* , **421**, 2001.
37. L. Patiny and A. Borel, *J. Chem. Inf. and Model.*, 2013, **53**, 1223.
38. J. A. Faniran and H. F. Shurvell, *Can. J. Chem.*, 1968, **46**, 2089.
39. T. G. Appleton, H. C. Clark and L. E. Manzer, *Coord. Chem. Rev.*, 1973, **10**, 335.
40. W. Henderson, S. Thwaite, B. K. Nicholson and T. S. A. Hor, *Eur. J. Inorg. Chem.*, 2008, 5119.
41. in *APEX-2. Bruker-Nonius AXS, Madison, Wisconsin, USA.*, Bruker AXS Editon edn., 2008.
42. L. Krause, R. Herbst-Irmer, G. M. Sheldrick and D. Stalke, *J. Appl. Cryst.*, 2008, **48**, 3.
43. G. M. Sheldrick, *Acta Cryst.*, 2015, **C71**, 3.
44. A. L. Spek, *Acta Cryst.*, 2009, **D65**, 148.

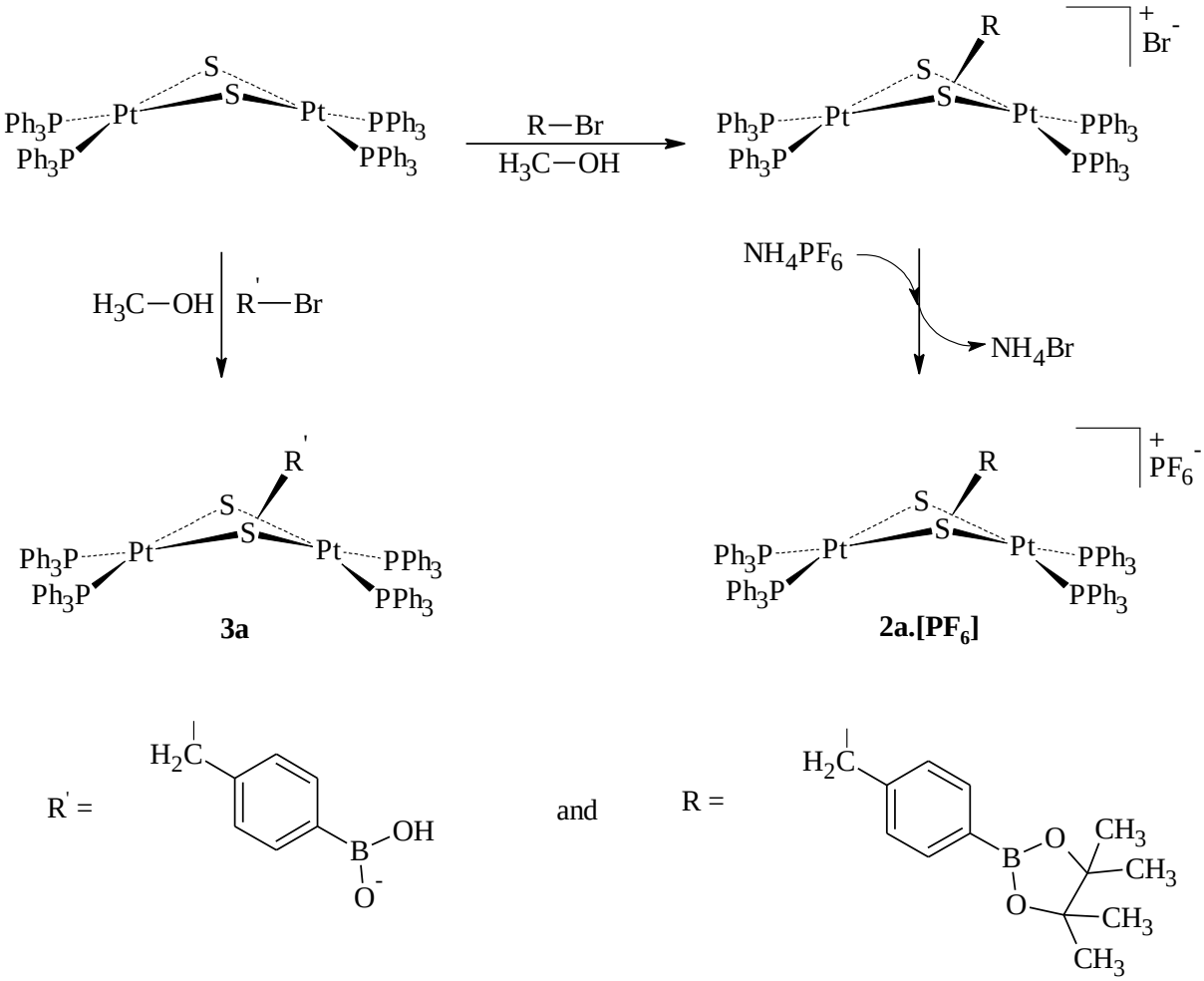

Scheme 1. The synthesis of monoalkylated complexes $[Pt_2(\mu\text{-}S)(\mu\text{-}SR)(PPh_3)_4]^+$, **2a·(PF$_6$)** and $[Pt_2(\mu\text{-}S)(\mu\text{-}SR')(PPh_3)_4]^+$, **3a**. R and R' = boronic acid pinacole ester and boronic acid moieties respectively.

Table 1. Selected bond lengths (Å) and angles (°) for $[Pt_2(\mu\text{-}S)\{\mu\text{-}CH_2(C_6H_4)B\{OC(CH_3)_2\}_2\}(PPh_3)_4](PF_6)$, **2a·(PF$_6$)**

Bond lengths and atomic distances (Å)			
Pt(1)-P(1)	2.3056(11)	Pt(1)-P(2)	2.2843(11)
Pt(2)-P(3)	2.3002(11)	Pt(2)-P(4)	2.2779(11)
Pt(1)-S(1)	2.3603(10)	Pt(1)-S(2)	2.3313(10)
Pt(2)-S(1)	2.3858(10)	Pt(2)-S(2)	2.3284(10)
S(1)-C(1)	1.829(5)	C(1)-C(2)	1.493(6)
O(1)-B(1)	1.365(7)	O(2)-B(1)	1.356(7)
Bond angles (°)			
P(1)-Pt(1)-S(2)	172.41(4)	P(2)-Pt(1)-S(1)	167.00(4)
P(4)-Pt(2)-S(1)	172.53(4)	P(3)-Pt(2)-S(2)	166.94(4)
S(1)-Pt(1)-S(2)	81.41(4)	S(2)-Pt(2)-S(1)	80.93(4)
C(1)-S(1)-Pt(1)	106.85(15)	C(1)-S(1)-Pt(2)	100.17(15)
Pt(2)-S(2)-Pt(1)	90.83(4)	Pt(1)-S(1)-Pt(2)	88.73(3)

Table 2. Selected bond lengths (Å) and angles (°) for $[Pt_2(\mu\text{-}S)\{\mu\text{-}S^+CH_2(C_6H_4)B(OH)(O^-)\}(PPh_3)_4]$, **3a**

Bond lengths and atomic distances (Å)			
Pt(1)-P(1)	2.296(2)	Pt(1)-P(2)	2.271(2)
Pt(2)-P(3)	2.282(2)	Pt(2)-P(4)	2.290(2)
Pt(1)-S(1)	2.366(2)	Pt(1)-S(2)	2.325(2)
Pt(2)-S(1)	2.346(2)	Pt(2)-S(2)	2.342(2)
S(1)-C(1)	1.836(10)	C(1)-C(2)	1.507(13)
Bond angles (°)			
P(1)-Pt(1)-S(2)	167.76(8)	P(2)-Pt(1)-S(1)	173.68(8)
P(4)-Pt(2)-S(1)	166.90(8)	P(3)-Pt(2)-S(2)	175.49(8)
S(1)-Pt(1)-S(2)	81.18(7)	S(2)-Pt(2)-S(1)	81.24(7)
C(1)-S(1)-Pt(1)	99.3(3)	C(1)-S(1)-Pt(2)	106.6(4)
Pt(2)-S(2)-Pt(1)	89.38(7)	Pt(1)-S(1)-Pt(2)	88.29(7)

Table 3: Crystallographic data for complex **2a·(PF$_6$)**.

Empirical formula	$C_{88}H_{84}BCl_6F_6O_2P_5Pt_2S_2$
Formula weight	2120.21
Temperature	120(2) K
Wavelength	0.71073 Å
Crystal system	Monoclinic
Space group	$P2_1/c$
Unit cell dimensions	a = 22.1024(15) Å α = 90°
	b = 15.4058(11) Å β = 104.8170(10)°
	c = 26.9561(19) Å γ = 90°
Volume	8873.5(11) Å^3
Z	4
Density (calculated)	1.587 g.cm^{-3}
Absorption coefficient (μ)	3.526 mm^{-1}
F(000)	4208
Crystal color, habit	colorless, block
Crystal size	0.232 × 0.120 × 0.106 mm^3
θ range for data collection	1.535 to 27.122°
Index ranges	$-28 \le h \le 28$, $-19 \le k \le 19$, $-34 \le l \le 34$
Reflections collected	158923
Independent reflections	19626 [R_{int} = 0.0371]
Completeness to θ = 25.242°	100.0 %
Absorption correction	Numerical
Max. and min. transmission	0.8210 and 0.5351
Refinement method	Full-matrix least-squares on F^2
Data / restraints / parameters	19626 / 42 / 1049
Goodness-of-fit on F^2	1.012
Final R indices [I>2σ(I)]	R_1 = 0.0346, wR_2 = 0.0885
R indices (all data)	R_1 = 0.0436, wR_2 = 0.0949
Largest diff. peak and hole	2.132 and -1.489 e$^-$.Å^{-3}

Table 4. Crystallographic data for complex **3a**

Empirical formula	$C_{79}H_{68}BO_2P_4Pt_2S_2$
Formula weight	1638.32
Temperature	120(2) K
Wavelength	0.71073 Å
Crystal system	Monoclinic
Space group	$P2_1/n$
Unit cell dimensions	a = 17.6538(16) Å α = 90°
	b = 23.694(2) Å β = 92.7640(10)°
	c = 20.1360(19) Å γ = 90°
Volume	8412.7(13) $Å^3$
Z	4
Density (calculated)	1.294 $g.cm^{-3}$
Absorption coefficient (μ)	3.486 mm^{-1}
F(000)	3240
Crystal color, habit	colorless, rod
Crystal size	0.185 × 0.061 × 0.035 mm^3
θ range for data collection	1.499 to 23.256°
Index ranges	$-19 \leq h \leq 19$, $-26 \leq k \leq 26$, $-22 \leq l \leq 22$
Reflections collected	107001
Independent reflections	12089 [R_{int} = 0.0765]
Completeness to θ = 23.256°	100%
Absorption correction	Numerical
Max. and min. transmission	0.09292 and 0.5336
Refinement method	Full-matrix least-squares on F^2
Data / restraints / parameters	12089 / 0 / 805
Goodness-of-fit on F^2	1.091
Final R indices [I>2σ(I)]	R_1 = 0.0468, wR_2 = 0.0958
R indices (all data)	R_1 = 0.0730, wR_2 = 0.1054
Largest diff. peak and hole	1.689 and -1.291 $e^-.Å^{-3}$

Table 5. A comparison of the geometric parameters [distances (Å) and angles (°)] for the complexes **2a·(PF_6), 3a, 4a·(BPh_4) and 5a·(PF_6) and 6a·(PF_6)** together with (estimated standard deviations are in parentheses where reported).

Parameter	**2a·(PF_6)**	**3a**	**4a·(BPh_4)**	**5a·(PF_6)**	**6a·(PF_6)**
Mean Pt–S	2.3299(10)	2.356(2)	2.3380(7)	2.339(3)	2.3343(17)
Mean Pt–SR	2.3731(10)	2.3335(2)	2.3716(7)	2.390(3)	2.3671(17)
Pt---Pt	3.319	3.282	3.282	3.297	3.325
S---S	3.060	3.052	3.087	3.071	3.077
Mean Pt–S–Pt	89.78(4)	88.84(7)	88.39(2)	88.44(8)	90.03(6)
Mean S–Pt–S	81.17(4)	81.21(7)	81.90(3)	81.02(9)	81.76(6)
Dihedral angle[a]	136.66	134.40	133.8	133.1	138.6

[a]Dihedral angle = angle between the S(1)–Pt(1)–S(2) and S(1)–Pt(2)–S(2) planes.

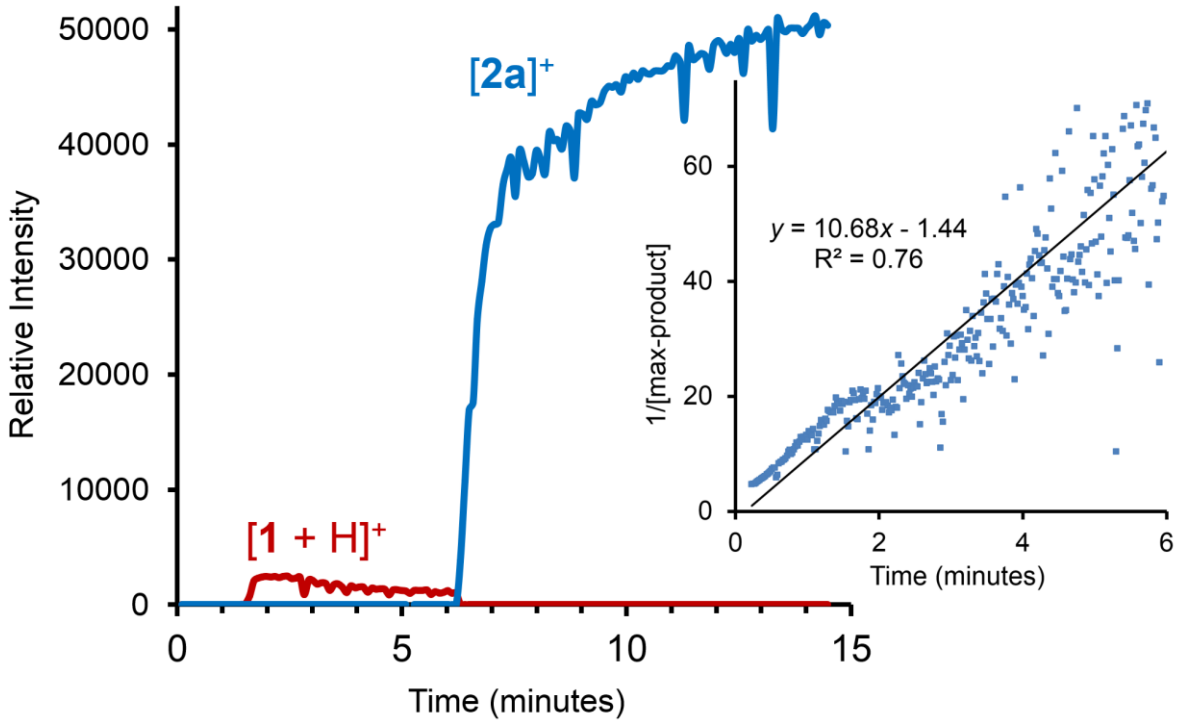

Figure 1. Intensities versus time for reaction of **1** and $BrCH_2(C_6H_4)B\{OC(CH_3)_2\}_2$ (injected at t = 6 minutes), measured using positive ion PSI-ESI-MS in methanol. Reaction is second order. Insert: plot of 1/[maximum intensity – product intensity] vs time since addition demonstrating that the production of $[\mathbf{2a}]^+$ follows second order kinetics.

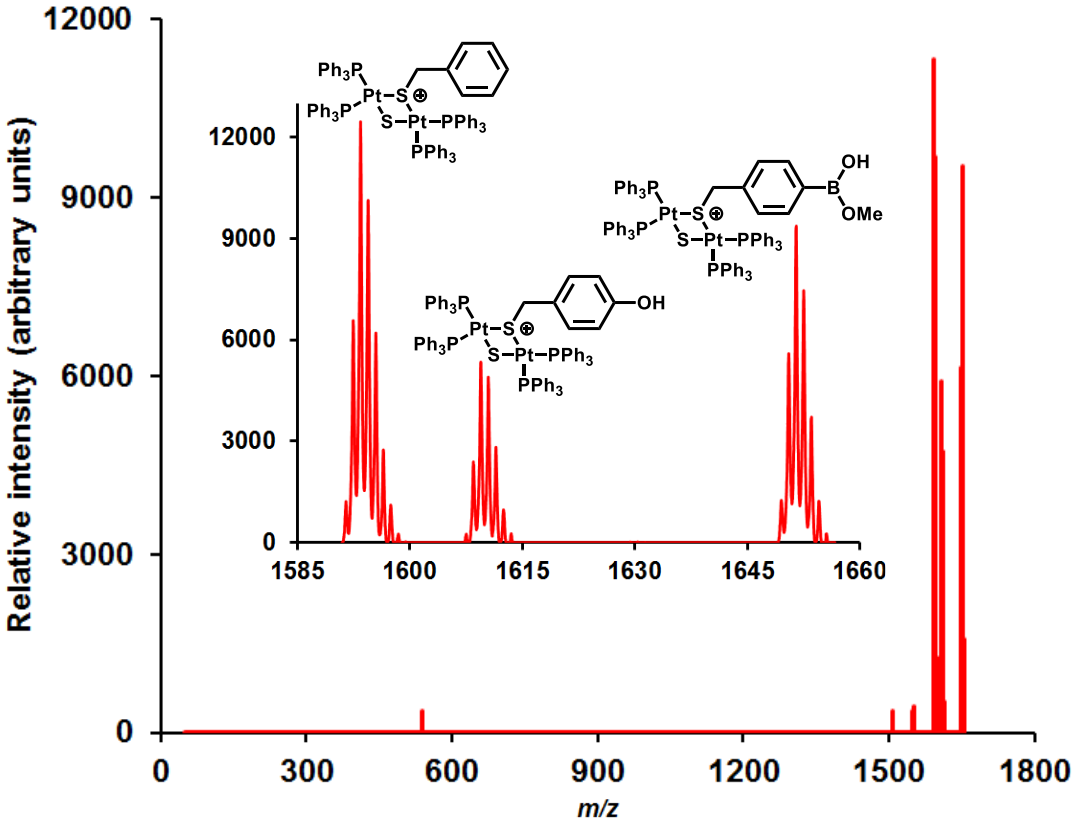

Figure 2. ESI-MS spectrum of the product isolated from the reaction of $[Pt_2(\mu\text{-}S)_2(PPh_3)_4]$ with $BrCH_2(C_6H_4)B(OH)_2$. Insert is an expansion of the region of interest.

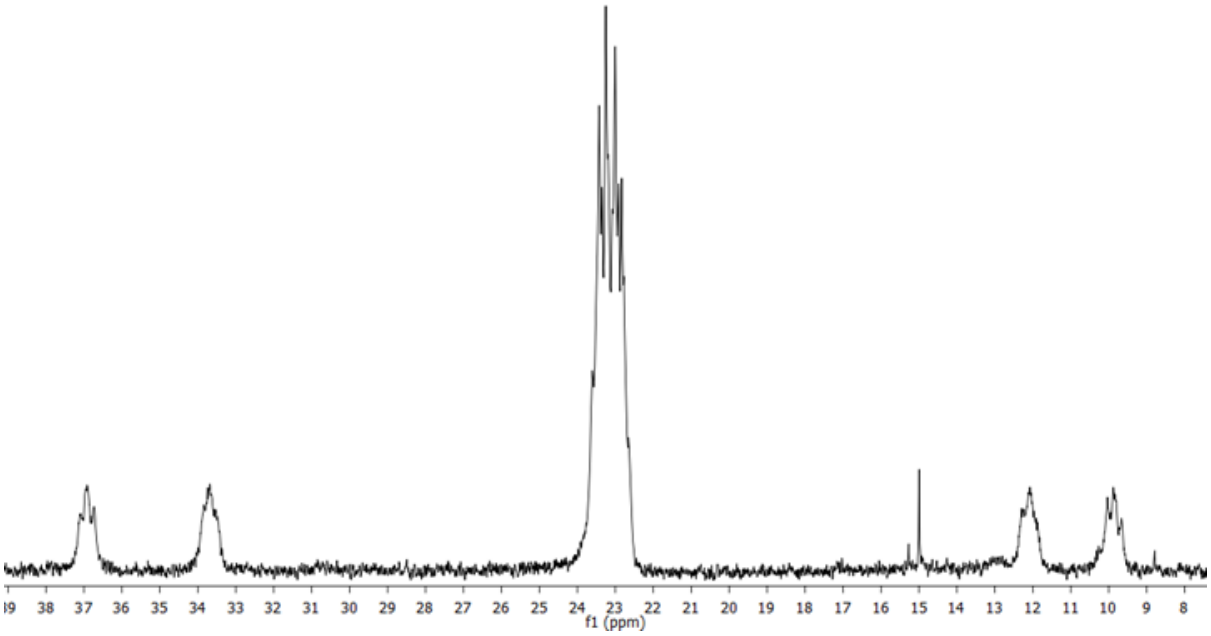

Figure 3. The $^{31}P\{^1H\}$ NMR spectrum of $[Pt_2(\mu\text{-}S)\{\mu\text{-}CH_2(C_6H_4)B\{OC(CH_3)_2\}_2\}(PPh_3)_4](PF_6)$, **2a·(PF$_6$)** showing the almost equivalence of the central peaks, with two sets of satellites due to different ^{195}Pt coupling constants.

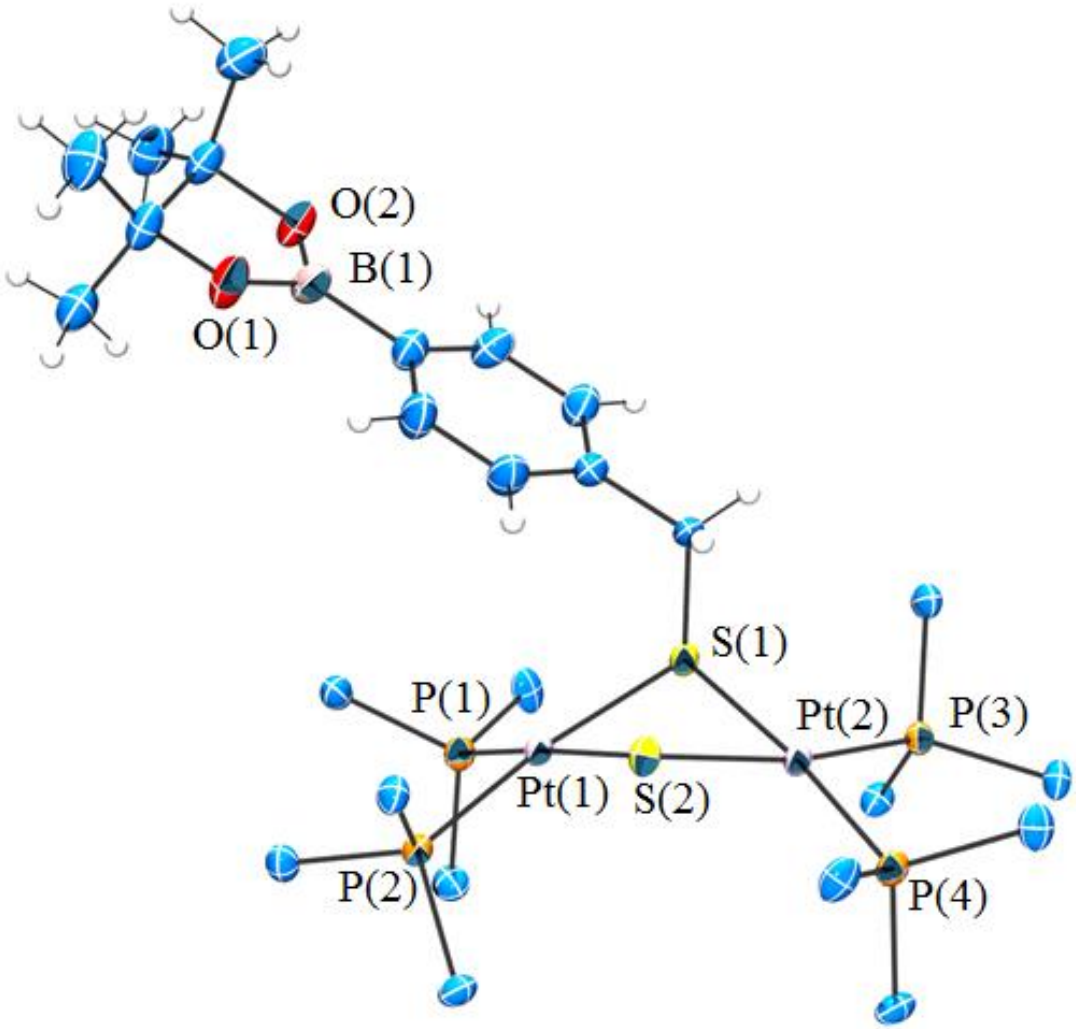

Figure 4. Molecular structure of the core of the complex $[Pt_2(\mu\text{-}S)\{\mu\text{-}SCH_2(C_6H_4)B\{OC(CH_3)_2\}_2\}(PPh_3)_4]^+$, **2a**, with only the ipso carbon atoms of the PPh_3 ligands shown.

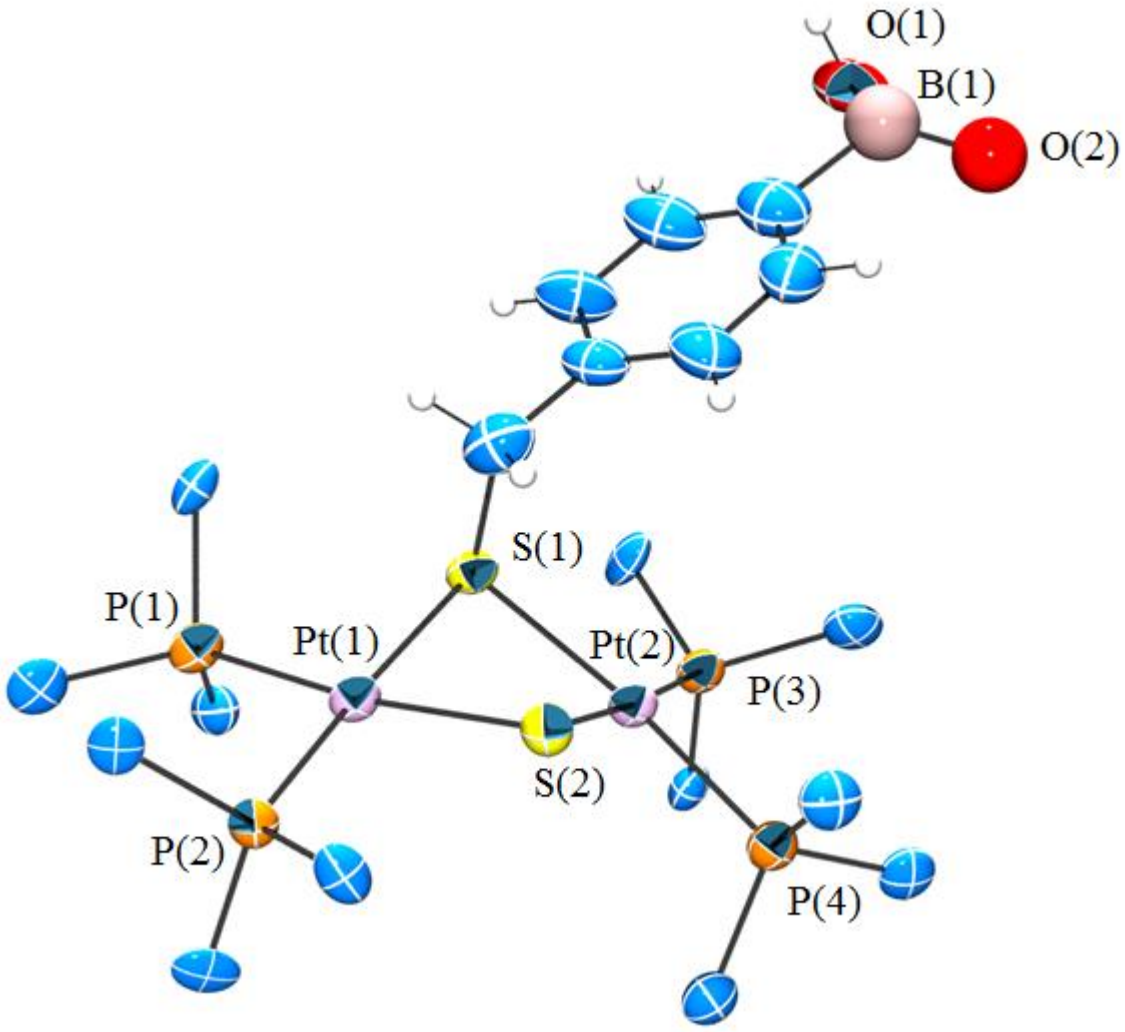

Figure 5. Molecular structure of the core of the complex $[Pt_2(\mu\text{-}S)\{\mu\text{-}S^{+}CH_2(C_6H_4)B(OH)(O^{-})\}(PPh_3)_4]$ **3a**, with only the *ipso* carbon atoms of the PPh_3 ligands shown.